Published in final edited form as:
Neurobiol Dis. 2013 February ; 50: 59–68. doi:10.1016/j.nbd.2012.10.003.

Critical role of neuronal pentraxin 1 in mitochondria-mediated hypoxic-ischemic neuronal injury

Md Al Rahim[a,b], **Shabarish Thatipamula**[a], and **Mir Ahamed Hossain**[a,b,*]

[a]Hugo W. Moser Research Institute at Kennedy Krieger, Baltimore, MD 21205, USA

[b]Department of Neurology, Johns Hopkins University School of Medicine, Baltimore, MD 21205, USA

Abstract

Developing brain is highly susceptible to hypoxic-ischemic (HI) injury leading to severe neurological disabilities in surviving infants and children. Previously, we have reported induction of neuronal pentraxin 1 (NP1), a novel neuronal protein of long-pentraxin family, following HI neuronal injury. Here, we investigated how this specific signal is propagated to cause the HI neuronal death. We used wild-type (WT) and NP1 knockout (NP1-KO) mouse hippocampal cultures, modeled *in vitro* following exposure to oxygen glucose deprivation (OGD), and i*n vivo* neonatal (P9-10) mouse model of HI brain injury. Our results show induction of NP1 in primary hippocampal neurons following OGD exposure (4–8h) and in the ipsilateral hippocampal CA1 and CA3 regions at 24–48 h post-HI compared to the contralateral side. We also found increased PTEN activity concurrent with OGD time-dependent (4–8h) dephosphorylation of Akt (Ser473) and GSK-3β (Ser9). OGD also caused a time-dependent decrease in the phosphorylation of Bad (Ser136), and Bax protein levels. Immunofluorescence staining and subcellular fractionation analyses revealed increased mitochondrial translocation of Bad and Bax proteins from cytoplasm following OGD (4h) and simultaneously increased release of Cyt C from mitochondria followed by activation of caspase-3. NP1 protein was immunoprecipitated with Bad and Bax proteins; OGD caused increased interactions of NP1 with Bad and Bax, thereby, facilitating their mitochondrial translocation and dissipation of mitochondrial membrane potential ($\Delta\Psi_m$). This NP1 induction preceded the increased mitochondrial release of cytochrome C (Cyt C) into the cytosol, activation of caspase-3 and OGD time-dependent cell death in WT primary hippocampal neurons. In contrast, in NP1-KO neurons there was no translocation of Bad and Bax from cytosol to the mitochondria, and no evidence of $\Delta\Psi_m$ loss, increased Cyt C release and caspase-3 activation following OGD; which resulted in significantly reduced neuronal death. Our results indicate a regulatory role of NP1 in Bad/Bax-dependent mitochondrial release of Cyt C and caspase-3 activation. Together our findings demonstrate a novel mechanism by which NP1 regulates mitochondria-driven hippocampal cell death; suggesting NP1 as a potential therapeutic target against HI brain injury in neonates.

*Corresponding Author: Mir Ahamed Hossain, Ph.D., Department of Neurology, The Kennedy Krieger Institute, 707 North Broadway, Room 400-N, Baltimore, MD 21205, Tel: 443-923-2678, Fax: 443-923-2695, hossain@kennedykrieger.org.

Keywords

Neuronal pentraxin 1; hypoxic-ischemic brain injury; oxygen glucose deprivation; mitochondria; Bax; Bad

Introduction

Brain injury due to fetal or neonatal asphyxia (Johnston, 1997; Lorenz et al., 1998; Northington et al., 2001a; Northington et al., 2001b;) or neonatal stroke is a leading cause of morbidity and mortality in surviving infants and children worldwide with a high societal cost (Balduini et al., 2004; Gresham et al., 1997; Shiber et al., 2010; Sudlow and Warlow, 1997; Volpe, 2001), and has an incidence as high as 1 in 4000 (Ferriero, 2004; Nelson, 2007). Yet, there is no promising therapy for neonatal brain injury at present; very few trials have documented limited clinical benefit (Blomgren and Hagberg, 2006; Kalenderian et al., 2009; Pezzini and Padovani, 2009; Uchino et al., 2001), in part, owing to incomplete understanding of the pathological secondary injury mechanisms that proceed from the primary insult (Blomgren et al., 2003; Blomgren and Hagberg, 2006; Pezzini and Padovani, 2009; Smaha, 2004). The hippocampus is often injured in neonatal stroke (Osredkar et al., 2010), and that disruption of oxygen and glucose supply resulting from occlusion of a blood vessel ultimately leads to neuronal losses and necrosis (Banasiak et al., 2000). Previously, we demonstrated the induction of a novel neuronal protein neuronal pentraxin 1 (NP1) in *in vivo* rat model of hypoxic-ischemic (HI) brain injury (Hossain et al., 2004), and that NP1 induction in HI cortical neuronal cell death is regulated via a glycogen synthase kinase (GSK)-3α/β-dependent mechanism (Russell et al., 2011). However, how this specific signal of NP1 induction is propagated to cause the HI neuronal death remains to be elucidated.

The cellular decision as to whether cells will undergo death or survival process is determined by the integration of multiple survival and death signals. The PI3-K/Akt signaling pathway plays a critical role in the survival of neuronal cells (Brunet et al., 2001). Whereas, PTEN (phosphatase and tensin homolog deleted on chromosome 10), which negatively regulates PI3-K/Akt pathway, plays a central role in cell migration, survival and apoptosis (Salmena et al., 2008) For example, PTEN deletion has been reported to prevent ischemic brain injury (Shi et al., 2011), and enhances regenerative ability of adult corticospinal neurons (Liu et al., 2010). In addition, there are many downstream effectors of PI3-K/Akt signaling pathway such as glycogen synthase kinase 3 (GSK-3) and Bcl-2/Bcl-xL-associated death protein (Bad) that play crucial roles in the process of cellular survival or deaths (Cross et al., 1995; Datta et al., 1997; del Peso et al., 1997; Hetman et al., 2000). In particular, GSK-3 is a critical activator of cell death in numerous models of neuronal apoptosis (Hetman et al., 2000; Li et al., 2000; Phiel et al., 2003), including HI (Russell et al., 2011). GSK-3β exerts some of its pro-apoptotic effects in neurons by regulating the mitochondrial localization of Bax, a key component of the intrinsic apoptotic cascade (Linseman et al., 2004).

Neuronal cell death signaling pathways in mitochondria has been demonstrated in the ischemic brain (Chan, 2004; Perez-Pinzon et al., 1999). This often occurs via an intrinsic cell death pathway triggered by the translocation of Bad and Bax, two proapoptotic Bcl-2 family members, to mitochondria (Armstrong and Jones, 2002; Yuan and Yankner, 2000; Zong et al., 2001), reduction in mitochondrial membrane potential ($\Delta\Psi_m$) (Deckwerth and Johnson, 1993), opening of the mitochondrial permeability transition pore (PTP) (Zarotti and Szabo, 1995), release of mitochondrial cytochrome *c* (Cyt C) (Narita et al., 1998; Wang et al., 1999; Zong et al., 2001) and formation of apoptosome with Apaf-1 and pro-caspase-9 leading to activation of the downstream executioner caspases, including caspase-3 (Li et al.,

1997a, 1997b; Zou et al., 1999). These findings suggest potential mitochondrion-targeted strategies for preventing HI neuronal cell death. In this study, we have used primary hippocampal neuronal cultures, modeled *in vitro,* following oxygen glucose deprivation and *in vivo* neonatal mouse model of HI to investigate the role of NP1 in causing cell death in the hippocampus, and also the underlying mitochondrial mechanisms of the NP1-mediated death program. Furthermore, we used NP1−/− primary hippocampal neurons to specifically demonstrate the contribution of NP1 in mediating mitochondrial perturbation and cell death.

Materials and methods

Mouse primary hippocampal culture and oxygen glucose deprivation

Primary hippocampal neuronal cultures were prepared from wild-type (WT), NP1 knockout (NP1-KO) mice (C57BL/6 background) and NP triple knockout (NP-TKO; all pentraxin family members-neuronal pentraxin 1, neuronal pentraxin 2 and neuronal pentraxin receptor are knocked down) mice (C57BL/6 and 129 mixed background) at postnatal day 1 or 2 (PND1 or 2) as described previously (Berbari et al., 2007) with modifications. NP1-KO and TKO mice were kindly provided by Dr. Paul Worley, Dept. of Neuroscience, School of medicine, Johns Hopkins University, Baltimore, MD, USA. After plating, at 2 days in vitro (DIV), half of the media were replaced with fresh medium additionally containing cytosine arabinofuranoside (AraC) to a final concentration of 5 μM to prevent non-neuronal proliferation. Thereafter, culture media was changed by half every 3 to 4 days. Cultures were used for experiments at 12–14 DIV. With this protocol, > 95% of cultured cells was MAP-2 (microtubule-associated protein-2) immunoreactive neurons (Chemicon, Temecula, CA) (Hossain et al., 2002).

To induce OGD, primary hippocampal neurons cultured at DIV 12–14 were placed in glucose-free Earl's balanced salt solution (EBSS) and exposed to humidified 95% N2/5% CO2 using anaerobic modular incubator chambers (Billups-Rothenberg, Del Mar, CA) for various time periods (4–8h) at 37ºC (Russell et al., 2011). Samples were collected immediately after OGD without any reoxygenation. Control cultures were placed in EBSS containing glucose and exposed to humidified 95% air/5% CO2 at 37ºC.

Unilateral cerebral hypoxia-ischemia

Common carotid artery (CCA) occlusion combined with controlled hypoxia in postnatal day 9–10 mouse pups was performed as described previously (Hossain et al., 2004) to produce hypoxic-ischemic brain injury. Briefly, under deep inhalant anesthesia (isofluorane in an oxygen-nitrous oxide mixture delivered via a Drager vaporizer), a 3–4 mm incision was made in the neck, and the right common carotid artery was isolated, double ligated, and cut between the ligatures. After the surgical procedure, the animals recovered for 2 h in a temperature-controlled incubator, and then animals were placed in an enclosed, vented 500 ml Plexiglas chamber that was partially submerged in 36°C water. Hypoxia was induced by continuous flow of warm, humidified gas (10% oxygen, balanced nitrogen) for 1 h. A subset of control animals were mock-treated with a small incision in their neck without CCA occlusion and placed in the Plexiglas chamber at normal air temperature (sham control). All procedures involving animals were performed in accordance with the NIH guide for the Care and Use of Laboratory Animals and were approved by The Johns Hopkins University Animal Care and Use Committee.

Assessment of cell cytotoxicity

Immediately after the indicated periods of exposure, cell cytotoxicity was determined by lactate dehydrogenase (LDH) assay. LDH released into the media after OGD exposure was measured using the Cytotoxicity Detection Kit (LDH) (Roche Diagnostics Corporation,

Indianapolis, IN, USA) as described previously (Hossain et al., 2004). Percent cell death was determined using the formula: % cytotoxicity = OGD LDH release (OD_{490}) / maximum LDH release (OD_{490}) after correcting for baseline absorbance of LDH release at 490 nm.

Immunofluorescence of the brain sections and neuronal cultures

Mouse pups were sacrificed at the indicated time-points after CCA ligation and hypoxia by perfusion fixation with ice-cold 4% paraformaldehyde in 1XPBS and then cryoprotected in 15% sucrose for overnight and then transferred to 30% sucrose solution for overnight followed by freezing with dry ice. Representative coronal brain sections (20 μm) from control and hypoxic–ischemic animals were immunostained as described previously (Hossain et al., 2004). Mouse monoclonal anti-NP1 (1:200) (BD Transduction Laboratories, Temecula, CA, USA) was used as the primary antibody, while donkey anti-mouse (1:200) Alexa fluor 568 is the secondary antibody (Invitrogen, Carlsbad, CA, USA). Immunofluorescence was visualized using an inverted fluorescence microscope (Olympus IX51fitted with DP2-DSW-V3.2 application software) at 10 X and ZEISS Axioimager M2 (AxioVision SE64 Rel.4.8.1 application software) at 100 X magnification.

Live immunostaining of primary hippocampal cultures (grown on coverslips) with NP1 was done as described previously with minor modifications (Hossain et al., 2004). Briefly, hippocampal neurons were live labeled with NP1 (1:100) for 45 min at 37° C. Neurons were then fixed with 3.7% formaldehyde, and permeabilized cells were stained with Alexa Fluor 568 (red)-conjugated anti-mouse secondary antibody (Invitrogen). For Cyt C-specific immunostaining, neurons were fixed with 3.7% formaldehyde followed by antigen retrieval using 5% urea in 0.1 M Tris/HCl at 95°C for 10 min. Thereafter, neurons were permeabilized and double labeled with Cyt C (1:100; BD Bioscience Pharmingen, San Diego, CA, USA) and VDAC (1:300; Abcam, Cambridge, MA, USA).

RNA isolation and real-time PCR

Total RNA was extracted using TRIzol reagent (Invitrogen) according to manufacturer's protocol. cDNA was synthesized from 1 μg of purified total RNA using iScript™ cDNA Synthesis Kit (Bio-Rad laboratories, Richmond, CA, USA), following the manufacturer's instructions. Quantitative real-time PCR was performed in triplicate by using iQ SYBR Green Supermix on CFX96™ Real-Time System (Bio-Rad). The mRNA level was normalized by housekeeping gene HPRT. The primers set used for NP1 were 5′-GCT GCG AGA GCC AGA GCA CC-3′ (sense) and 5′-TTG CCC GAG TTG GCT GAG CG-3′ (anti-sense), and for HPRT were 5′-CCT GGC GTC GTG ATT AGT GAT G-3′ (sense) and 5′-CAG AGG GCT ACA ATG TGA TGG C-3′ (anti-sense).

SDS-PAGE and Western blot analyses

Western blotting was performed with standard methods as described previously (Hossain et al., 2011). Cultured neurons were exposed to OGD or mouse hippocampal tissues were collected at the indicated time-points after HI. Whole cell lysates or the proteins extracted from the tissue were subjected to Western blot analysis. Blots were probed with primary antibodies for NP1 (1:1000, BD Transduction Laboratories), PTEN (1:1000, Cell Signaling, Beverly, MA, USA), phospho-Akt (s473) (1:1000, Cell Signaling), phospho-GSK-3β (1:1000, Cell Signaling), GSK-3β (1:1000, Cell Signaling), phospho-Bad (s136) (1:1000, Cell Signaling), Bax (1:1000, Cell Signaling), Cyt C (1:1000; BD Biosciences Pharmingen), procaspase-3 and cleaved caspase-3 (1:1000; Cell Signaling), VDAC (1:1000, Abcam) and β-actin (1:5000, Sigma, St. Louis, MO, USA). Horseradish peroxidase (HRP)-conjugated secondary antibodies (GE Healthcare, Piscataway, NJ, USA) were used at 1:5000 dilutions for 1 h at RT. HRP reaction product was then visualized by enhanced chemiluminescence

using an ECL Western blotting detection kit (Pierce, Rockford, IL, USA). Digitized images were quantified using NIH ImageJ software.

Preparation of cytosolic and mitochondrial fractions

Subcellular fractionation was performed as described previously (Russell et al., 2008; Sharma et al., 2011). Briefly, cell pellets were homogenized in isotonic MB (mitochondrial buffer) consisting of 210 mM mannitol, 70 mM sucrose, 1 mM EDTA and 10 mM Hepes, pH 7.5, supplemented with protease and phosphatase inhibitor cocktails (Calbiochem, San Diego, CA, USA) followed by centrifugation at 500 g for 5 min. The pellet is the nuclear fraction. The post-nuclear supernatant was centrifuged at 10,000 g for 30 min at 4°C for the mitochondrial fraction. The pellet containing the mitochondrial fraction was suspended in 50 μl of MB containing 0.1% Triton X-100 to break up the mitochondria; the supernatant was used as the crude cytosolic fraction. To confirm the separation of cytosolic and mitochondrial fractions, blots were stripped and incubated with actin and VDAC, respectively, which also served as a loading control.

Coimmunoprecipitation of NP1 with Bad and Bax

After exposure of the cells to the conditions as indicated in the figure legends, total cellular extracts from hippocampal cultures were prepared in immunoprecipitation buffer (10 mM sodium phosphate, 100 mM NaCl, 1% Triton X-100) containing 1X protease inhibitor cocktail set, and phosphatase inhibitor cocktail (Calbiochem) following the method as described previously (Hossain et al., 2004). One hundred micrograms of total proteins were subjected to immunoprecipitation by incubation overnight with Bad (1:100, Cell Signaling) and Bax (1:100, Cell Signaling) at 4 °C with constant shaking. Then, 20 μl of protein A/G-agarose conjugated beads (Santa Cruz Biotechnology, Inc., Santa Cruz, CA, USA) was added to each sample and incubated for 2–4 hr at 4°C. The beads were collected, washed, and boiled for 3 min in 50 μl of 1 X electrophoresis sample buffer followed by Western blot analysis.

Mitochondrial membrane potential

Mitochondrial membrane potential, $\Delta\Psi_m$ (delta psi), was measured using a JC-1 kit (Molecular Probes, Eugene, OR, USA) following manufacturer's protocol. Briefly, cells were incubated with 1.5 μM of JC-1 (5,5′,6,6′-tetrachloro-1,1′,3,3′-tetraethyl-benzimidazolylcarbocyanine iodide) for 15 min at 37°C. After incubation, cells were washed once with PBS, and images were obtained using an inverted fluorescent microscope (Olympus IX51) fitted with a DP-72 digital color camera.

Statistical analysis

Statistics were performed using GraphPad Prism software, Version 5.01. For one experimental and one control group, two-tailed Student's t-test was used to determine if differences exist between means. Comparisons involving multiple groups were done by ANOVA, followed by Bonferroni/Dunn post-hoc test where appropriate. Significance level was assigned at $P<0.05$.

Results

NP 1 is induced in dissociated primary hippocampal cultures exposed to OGD and in the hippocampus of neonatal mice following HI brain injury

Hippocampal brain regions are highly susceptible to injury in the event of stroke (Osredkar et al., 2010). First, we asked whether NP1 is contributing to the neuronal death in the hippocampus. We used mature hippocampal cultures (12-14 DIV) to investigate OGD-

induced neuronal death, because of the higher degree of sensitivity of mature hippocampal neurons (12-18 DIV) to hypoxic damage (Loreto and Balestrino, 1997). Increased induction of NP1 mRNA and protein levels were observed after exposure of primary hippocampal neurons to OGD. Quantification of NP1 mRNA and protein levels revealed an OGD time-dependent increase with more than two-fold induction observed at 4 h of exposure, which reached the maximum at 8 h (approximately 4 fold), compared to the normoxic control cultures (Fig. 1A & B). We used 4 h time point of OGD exposure in subsequent experiments as we observed clear evidence of injury following 4 h of OGD exposure in WT hippocampal neurons, similar to that we reported previously (Russell et al., 2011). Our immunocytochemical experiments showed enhanced NP1-specific immunostaining of the hippocampal neurons after OGD exposure (4 h) compared to the normoxic control cultures (Fig. 1C), further confirming the induction of NP1 protein in response to OGD exposure. Comparing the time-course of NP1 induction and the appearance of characteristic features of neuronal death, it appears that NP1 induction is an early event, and that the induction occurs before actual cell death. To further confirm NP1 induction in hippocampal neurons, next we immunostained brain sections from WT neonatal mouse HI brains. Fluorescence microscopy showed enhanced NP1-specific immunoreactivity in the ipsilateral hippocampus, which was localized in the pyramidal layer of CA3 and CA1 regions, but not in the dentate gyrus (DG) 48 h after HI onset (Fig. 1D, top). Further analysis of brain sections by fluorescence microscopy of the HI brain sections revealed intense NP1-specific fluorescence associated with individual neurons in the hippocampal regions (inset). Western analyses of the hippocampus tissue homogenate also showed a time-dependent increase in the NP1 protein levels after HI (24 & 48 h) compared to the sham controls (Fig. 1D, bottom); corroborating the induction of NP1 in the hippocampus after HI injury.

Hippocampal neurons from NP1-KO and NP-TKO mice, but not from WT, are protected against OGD exposure

To correlate between NP1 induction and cell death in hippocampal cultures, we measured cell cytotoxicity by lactate dehydrogenase (LDH) activity assay following OGD exposure. Quantification of LDH release showed an OGD-induced increase in hippocampal cell death (Fig. 2A), which is consistent with our previous reports showing hypoxia-induced cell death in primary cortical neurons (Hossain et al., 2004; Russell et al., 2011). Cell cytotoxicity was evident by an increase in LDH release (~3-fold at 6h post-OGD) compared to the normoxic control cultures.

To directly demonstrate the link between NP1 induction and cell death, we used hippocampal neurons from both NP1-KO and NP-TKO mice, and exposed them to identical OGD conditions. Our cytotoxicity results showed very negligible change in the release of LDH in NP1-KO and NP-TKO neurons after exposure to OGD compared to the controls (Fig. 2A). Our results suggest that neurons from both NP1-KO and NP-TKO mice are significantly protected from OGD compared to the WT cultures, as evidenced by decreased LDH release. Also, light microscopic analysis showed characteristic changes of dying cells with disintegration of processes and cell bodies in WT hippocampal neurons following OGD (Fig. 2B). In contrast, both NP1-KO and NP-TKO neurons were significantly protected from OGD compared to the neurons from WT mice, which retained morphological features of a healthy neuron, such as larger cell bodies, phase brightness and intact processes.

Activation of PTEN with consequent dephosphorylation of Akt in OGD exposed hippocampal neurons is associated with GSK-3β-induced NP1 expression

Exposure of hippocampal neurons to OGD time-dependently decreased the phosphorylation of PTEN with a small increase in the PTEN protein levels, drastically dephosphorylated Akt (Supplemental Fig. 1), which is in agreement with our previous reports (Russell et al., 2011).

We also found significant dephosphorylation of GSK-3β at 4 h, and complete dephosphorylation occurred beyond 4 h of OGD exposure (6–8 h) (Fig. 3A), suggesting the activation of GSK-3β under such conditions. Interestingly in NP-TKO (Fig. 3B) and NP1-KO (Fig. 3C) neurons, the pGSK-3β levels remained unchanged up to 4 h OGD compared to respective normoxia control, however, a delayed dephosphorylation (i.e. activation) of the kinase was observed at 6–8 h of exposure. It is worth noting that we found no significant difference in pGSK-3β protein levels between the WT and KO neurons under control normoxia condition. We also observed no change in β-actin protein levels, used as an internal control, across the all experimental time points examined. The blockade of GSK-3 activity by using GSK-3-specific inhibitor SB216763 revealed significant inhibition of NP1 expression (Fig. 3D) and neuronal death (Fig. 3E) compared to that observed in SB216763 untreated OGD group (Fig. 3D-E). Our results clearly show GSK-3β signaling is contributing to NP1-induced hippocampal cell death following OGD exposure.

OGD caused differential expression of Bax and phospho-Bad levels in WT and NP1-KO hippocampal cultures

It is known that Akt phosphorylates Bad and blocks the Bad-induced death of primary neurons by blocking its translocation the mitochondria (Datta et al., 1997). Also, GSK-3β exerts some of its pro-apoptotic effects in neurons by regulating the mitochondrial localization of Bax (Linseman et al., 2004). Here, we examined the Bax protein levels, and phosphorylation of Bad (at Ser136) under similar OGD conditions in WT and NP1-KO cultures. Western blot analysis using phospho-specific Bad primary antibody showed that phosphorylation of Bad (Ser136) drastically reduced at 4 h of OGD insult with essentially complete disappearance after 8 h in WT neurons (Fig. 4A, top); whereas, in NP1-KO cultures, no change in phospho-Bad protein levels was detected, at least, up to 4h of OGD exposure. However, a much delayed and less pronounced dephosphorylation of Bad was observed after 6h (Fig. 4B, top). We also found that the Bax protein levels were decreased in WT hippocampal neurons after OGD exposure (4 to 8h) (Fig. 4A, bottom panels). In contrast, there was no change in the Bax protein levels in NP1-KO cultures up to 4–6h of OGD exposure, although Bax was decreased after 6 h (Fig. 4B, bottom panels). However, the basal levels of phospho-Bad and Bax protein were found to be comparable between WT and NP1-KO groups. These results, therefore, indicate that a differential distribution of the proapoptotic Bad and Bax proteins might have ensued in WT and NP1-KO cultures between the cytosolic and mitochondrial compartments in the event of OGD exposure.

NP1 associates with Bad and Bax proteins in a GSK-3-dependent manner to facilitate their mitochondrial translocation and trigger mitochondrial release of Cyt C

Dephosphorylation of Bad allows it to get translocated from the cytosol to the mitochondria where the protein initiates Cyt C release to promote apoptosis (Shou et al., 2004; Wang et al., 1999). Also, GSK-3β plays a role in the translocation of Bax to the mitochondria (Banasiak et al., 2000; Linseman et al., 2004; Narita et al., 1998). To examine OGD-induced mitochondrial translocation of Bad and Bax and release of Cyt C in WT and NP1-KO hippocampal neurons, we performed subcellular fractionations followed by Western blotting analyses (Russell et al., 2008; Sharma et al., 2011). In cytosolic fractions, significantly decreased levels of Bad (~ 70%; $p<0.05$) and Bax (~ 58%; $p<0.01$) were observed with concurrent increase in Cyt C protein level (~ 6-fold; $p<0.001$) in the OGD exposed WT neurons compared to the normoxia controls. On the other hand, in the mitochondrial fractions Bad (~ 4-fold; $p<0.05$) and Bax (~2-fold; $p<0.01$) levels were increased significantly with simultaneous decrease of Cyt C protein level (~ 75%; $p<0.01$) after OGD exposure compared to the normoxia controls. These results suggest increased mitochondrial translocation of Bad and Bax after OGD exposure (4 h) of WT hippocampal neurons with consequent mitochondrial release of Cyt C into the cytoplasm (Fig. 5A). In contrast, no

significant changes of Bad, Bax and Cyt C levels were observed in both the cytoplasmic and mitochondrial fractions from NP1-KO hippocampal neurons following OGD exposure compared to that in control normoxia NP1-KO cultures. Thus, it appears that OGD exposure could not trigger the translocation of Bad and Bax from cytosol to mitochondria in NP1-KO neurons (Fig. 5B). Our results clearly demonstrate a role of NP1 in mitochondrial localization of Bad and Bax following OGD.

To directly demonstrate the association of NP1 with Bad and Bax proteins, and the role of GSK-3 in the interaction between NP1 and Bad/Bax, we performed complementary co-immunoprecipitation experiments with or without SB216763 (10 μM) pretreatment using Bad- and Bax- specific primary antibodies. Our results showed that NP1 was co-precipitated with both Bad (Fig. 5C) and Bax (Fig. 5D) proteins, and increased precipitation of NP1 was observed after OGD exposure, whereas pretreatment with GSK-3 inhibitor blocked the NP1/Bad and NP1/Bax associations. These results clearly show that NP1 forms protein complexes with Bad and Bax proteins which is GSK-3β-dependent, and that OGD enhances NP1 interactions with Bad and Bax to facilitate their mitochondrial localization.

NP1 contributes to OGD-induced dissipation of mitochondrial membrane potential ($\Delta\Psi_m$), and subsequent Cyt C release, caspase-3 activation and cell death

Translocation of Bcl-2 pro-apoptotic proteins, including Bad and Bax, to the mitochondria leads to loss of mitochondrial membrane potential ($\Delta\Psi_m$) (Armstrong and Jones, 2002), which is an early episode in several instances of apoptosis (Green and Reed, 1998). Next, we investigated the change in $\Delta\Psi_m$ in both WT and NP1-KO cultures at an earlier time-point of OGD (2h) by using a cationic membrane potential indicator JC-1. In healthy cells, the dye stains the mitochondria bright red. Whereas in apoptotic cells, the JC-1 dye cannot accumulate in the mitochondria and remains in the cytoplasm in a green fluorescent monomeric form (Cossarizza et al., 1993). Exposure of WT neurons to OGD showed drastic decrease in red fluorescence, which is a measure of $\Delta\Psi_m$ loss, after 2h of OGD relative to unexposed control cultures (6A, top). The normalized JC-1 fluorescence (red-to-green ratio) showed significant decrease (~65% decrease; $p<0.001$) following OGD of the hippocampal neurons compared to the normoxic controls. Importantly in NP1-KO cultures, there was no significant change in the JC-1 fluorescence, i.e. red-to-green ratio, between the control and OGD groups (Fig. 6A bottom). Mitochondria in both groups exhibited yellow appearance, suggesting no significant loss of $\Delta\Psi_m$.

Next, we examined the subcellular localization of Cyt C in WT and NP1-KO neurons after OGD by immunofluorescence using Cyt C-specific antibody as described previously (Russell, 2008). WT neurons exposed to OGD exhibited pronounced Cyt C release, as evidenced by the presence of red fluorescence in the cytoplasm (Fig. 6B top right). In contrast, there was no evidence of Cyt C (red) fluorescence in the cytoplasm after exposure of NP1-KO neurons to OGD. Cyt C remained mostly in the mitochondria (Fig. 6B bottom right), which appears as yellow i.e. Cyt C-specific immunofluorescence being overlapped with mitochondrial marker VDAC. Mitochondrial release of Cyt C triggers procaspase-3 proteolysis/activation to mediate the caspase-mediated cell death (Budd et al., 2000). In agreement with this, we found that cleaved (activated) caspase-3 was significantly increased in WT cultures after OGD compared to the control cultures (Fig. 6C left). There was also a decrease in the procaspase-3 level following OGD in WT cultures compared to the normoxic controls. However, activation of caspase-3 has also been reported without change in procaspase-3 protein levels in neuronal death in similar neonatal rodent models of HI (Namura et al., 1998; Nakajima et al, 2000). In contrast, levels of cleaved caspase-3 were comparable between the control and OGD groups in NP1-KO neurons (Fig. 6C right). Our results, thus, clearly demonstrate the involvement of NP1 in mediating mitochondria-driven prodeath caspase pathways. In a separate study we also observed increased NP1 induction in

neurons of HI brain sections, which also showed enhanced cleaved caspase-3 (+) immunoreactvity (unpublished data), further supporting the involvement of NP1 in mitochondria-mediated neuronal death.

Discussion

The present study demonstrates induction of NP1 in primary hippocampal neuronal cultures following OGD and in the ipsilateral hippocampal CA1 and CA3 areas following HI in neonatal mice, and further delineates how induction of NP1 is involved in mediating neuronal death. Firstly, OGD caused activation of PTEN with subsequent dephosphorylation of Akt (i.e. inactivation), and prodeath kinase GSK-3β (i.e. activation) in WT hippocampal cultures. Secondly, OGD induced down-regulation of Bax and decreased phosphorylation of Bad that resulted in enhanced mitochondrial translocation of the Bax and Bad proteins. This was also evident by the dissipation of $\Delta\Psi_{m,}$ increased mitochondrial release of Cyt C with subsequent activation of caspase -3 ultimately leading to neuronal death. Particularly interesting is our identification of the association of NP1 with the prodeath proteins Bad and Bax, which further facilitated Bax and Bad mitochondrial localization and OGD-induced neuronal death. Thirdly, in contrast to the WT cultures, the NP1−/− null hippocampal cultures showed no significant change in mitochondrial translocation of Bad and Bax, $\Delta\Psi_{m}$, and no apparent increase in mitochondrial release of Cyt C and caspase-3; resulting in significant protection of the NP−/− neurons against the OGD insult. This is the first demonstration of significant neuroprotection in NP1-KO hippocampal neuronal cultures under ischemic stroke condition, further supporting a crucial role of NP1 in neuronal death.

The brain is mostly susceptible to oxidative stress because it consumes a large quantity of oxygen, and hippocampus, in particular, is often vulnerable in hypoxia-ischemia (Osredkar et al., 2010). Previous report from our laboratory showed NP1 induction in hypoxic-ischemic brain injury (Hossain et al., 2004), and GSK-3α/β regulated the expression of the NP1 in cultured cortical neurons (Russell et al., 2011). In this study, we show the specificity of NP1 induction in OGD-induced neuronal death using a homogenous population of mature hippocampal neuronal cultures. We also found HI-time dependent induction of NP1 in the hippocampal (pyramidal layers of CA3 and CA1) regions; the same brain areas that developed infarction (i.e. injury) following HI. In fact, NP1 induction occurred prior (24 h and prior) to the development of the infarction (data not shown), indicating NP1 as an upstream component of the death cascade. This was evidenced by OGD time-dependent expression of NP1 mRNA and protein in cultured hippocampal neurons and the observed OGD-induced neuronal death. Live immunostaining of hippocampal neurons with NP1 antibody further consolidated our findings that NP1 induction occurs before the actual cell death. In addition, the intact morphological characteristics and significantly less cell death observed in NP1-KO and NP-TKO neurons following OGD specifically establish a role of NP1 inhibition in neuroprotection. Taken together our results provide strong evidence that NP1 induction plays a key role in OGD-induced hippocampal neuronal death.

Ample evidence suggests that apoptotic and anti-apoptotic signaling pathways are activated after cerebral HI, and that a shift in the balance between apoptotic and anti-apoptotic cellular factors determines cells fate. The PI3-K/Akt pathway regulates the survival response against pro-apoptotic stimuli (Cross et al., 1995; Hetman et al., 2000), whereas, PTEN, which acts as an antagonist of PI3-K (Oudit et al., 2004) has been reported to play a role in mediating mitochondria-dependent apoptosis (Zhu et al., 2006) and ischemic brain damage (Ning et al., 2004). We found OGD time-dependent decrease in the phosphorylation of PTEN and Akt, abolishing their protective effects. Whereas, decrease in the phosphorylation of the downstream target GSK-3β results in activation of the death kinase, which is consistent with previous reports (Enguita et al., 2005; Russell et al., 2011). Similarly, blockade of GSK-3

activity by pharmacological inhibitor decreased the OGD-induced expression of NP1 and its interaction with Bad and Bax, further supporting the GSK-3-dependent induction of NP1. Interestingly, the activation of GSK-3β appears to be suppressed in NP-KO cultures, at least during the early time-points of OGD. This is possibly because of the fact that knock down of NP1 gene is neuroprotective- a condition where prosurvival PI3-K/Akt pathways are active that may have contributed to the observed phosphorylation of GSK-3β (inactivation), shifting the balance toward the survival path.

The Bcl-2 family of proteins Bad and Bax play a crucial role in intracellular apoptotic signal transduction by regulating the permeability of mitochondrial membrane (Yuan and Yankner, 2000; Zong et al., 2001). Akt phosphorylates Bad (Datta et al., 1997) and phosphorylation of Bad promotes binding to 14-3-3 proteins to be sequestered in the cytosol (Datta et al., 2000; Yang et al., 1995; Zha et al., 1996). Thus, Akt deactivation and decreased phosphorylation of Bad following OGD resulted in enhanced mitochondrial localization of Bad. Similarly, Bax translocation to mitochondria triggers neuronal apoptosis (Zong et al., 2001). Bax is a direct target of GSK-3β that modulates Bax expression and function at the transcriptional and posttranslational levels to promote mitochondrial apoptosis (Linseman et al., 2004; Watcharasit et al., 2003). Our findings suggest that activated GSK-3β following OGD resulted in decreased Bax protein levels in the cytoplasm with concurrent increase in the mitochondrial fraction. Importantly, OGD exposure of NP1−/− null hippocampal neurons did not display any change in Bax protein and phospho-Bad levels. Also, knockdown of NP1 prevented the translocation of Bad and Bax from cytosol to mitochondria; indicating a specific involvement of NP1 in mitochondrial localization of Bad/Bax proteins following OGD.

The cell death signaling pathway in mitochondria has been demonstrated in the ischemic brain and that mitochondrial membrane depolarization and Cyt C release from inner membrane determine the final steps of apoptosis (Merry and Korsmeyer, 1997; Narita et al., 1998). Mitochondrial membrane potential is a very important marker for the function of mitochondria and a decrease in $\Delta\Psi_m$ predicts cell injury (Green and Reed, 1998). To specifically demonstrate the role of NP1 in reduction of $\Delta\Psi_m$, we found that NP1-KO cultures resisted the OGD-induced dissipation of $\Delta\Psi_m$ and there was significant inhibition of mitochondrial release of Cyt C. While we cannot rule out the contribution of other stressors on OGD-induced mitochondrial outer membrane permeabilization, our results clearly showed stabilization and neuroprotection from mitochondrial cell death pathway as a specific characteristic of NP1-KO hippocampal neurons. Most interestingly, our co-immunoprecipitation experiments revealed that NP1 formed protein complexes with Bad and Bax, and that OGD caused an increase in the interactions of both NP1-Bad and NP1-Bax. However, the increased association of NP1/Bad and NP1/Bax following OGD was reversed by pretreatment with SB216763, which further confirmed the GSK-3 regulation on NP1 expression and ensuing interactions with Bad and Bax proteins. Our current results are also in agreement with the report that shows NP1 facilitates the accumulation of Bax in mitochondria during apoptosis in cerebellar granule neurons in culture (Clayton et al., 2012). Therefore, we suggest that NP1 influences the translocation of these proapoptotic proteins to the mitochondria, thereby contributing to mitochondrial outer membrane permeabilization. We also observed cell death after OGD was associated with robust increase in activated caspase-3 in WT neurons but not in the NP1-KO cultures under identical condition, supporting a role for NP1 in mitochondria-mediated caspase-3-dependent cell death pathway as evident by LDH release in WT vs. NP1-KO neurons. It appears that absence of NP1 desensitizes neurons to the ischemic injury by preventing mitochondria-mediated activation of cell death pathway.

In summary, our results clearly demonstrate a mechanism (Fig. 7) by which NP1 influences mitochondria-mediated cell death by facilitating the translocation of proapoptotic Bad and Bax proteins to the mitochondria, decreasing $\Delta\Psi_m$ and releasing Cyt C into the cytosol with subsequent activation of caspase-3. Our results present a novel mechanism of neuronal death involving PTEN/PI3K/Akt/GSK-3-dependent NP1 induction and its contribution to mitochondria-mediated hippocampal neuronal death following HI insult. Taken together, our findings suggest a novel neuroprotective strategy in neonates suffering from HI brain injury.

Supplementary Material

Refer to Web version on PubMed Central for supplementary material.

Acknowledgments

We gratefully acknowledge Dr. Paul Worley for providing the knockout mice. This work was supported by the National Institutes of Health grant RO1 NS046030 and the Cerebral Palsy International Research Foundation grant R-793-09.

References

Armstrong JS, Jones DP. Glutathione depletion enforces the mitochondrial permeability transition and causes cell death in Bcl-2 overexpressing HL60 cells. FASEB J. 2002; 16:1263–1265. [PubMed: 12060676]

Balduini W, Carloni S, Mazzoni E, Cimino M. New therapeutic strategies in perinatal stroke. Curr Drug Targets CNS Neurol Disord. 2004; 3(4):315–23. [PubMed: 15379607]

Banasiak KJ, Xia Y, Haddad GG. Mechanisms underlying hypoxia-induced neuronal apoptosis. Prog Neurobiol. 2000; 62:215–249. [PubMed: 10840148]

Berbari NF, Bishop GA, Askwith CC, Lewis JS, Mykytyn K. Hippocampal neurons possess primary cilia in culture. J Neurosci Res. 2007; 85:1095–1100. [PubMed: 17304575]

Blomgren K, Zhu C, Hallin U, Hagberg H. Mitochondria and ischemic reperfusion damage in the adult and in the developing brain. Biochem Biophys Res Commun. 2003; 304(3):551–9. [PubMed: 12729590]

Blomgren K, Hagberg H. Free radicals, mitochondria, and hypoxia-ischemia in the developing brain. Free Radic Biol Med. 2006; 40(3):388–97. [PubMed: 16443153]

Brunet A, Datta SR, Greenberg ME. Transcription-dependent and -independent control of neuronal survival by the PI3K-Akt signaling. Curr Opin Neurobiol. 2001; 11:297–305. [PubMed: 11399427]

Budd SL, Tenneti L, Lishnak T, Lipton SA. Mitochondrial and extramitochondrial apoptotic signaling pathways in cerebrocortical neurons. Proc Natl Acad Sci USA. 2000; 97:6161–6166. [PubMed: 10811898]

Chan PH. Mitochondria and neuronal death/survival signaling pathways in cerebral ischemia. Neurochem Res. 2004; 29:1943–1949. [PubMed: 15662830]

Clayton KB, Podlesniy P, Figueiro-Silva J, et al. NP1 regulates neuronal activity-dependent accumulation of Bax in mitochondria and mitochondrial dynamics. J Neurosci. 2012; 32:1453–66. [PubMed: 22279230]

Cossarizza A, Baccarani-Contri M, Kalashnikova G, Franceschi C. A new method for the cytofluorimetric analysis of mitochondrial membrane potential using the J-aggregate forming lipophilic cation 5,5′,6,6′-tetrachloro-1,1′,3,3′-tetraethylbenzimidazolcarbocyanine iodide (JC-1). Biochem Biophys Res Commun. 1993; 197(1):40–45. [PubMed: 8250945]

Cross DA, Alessi DR, Cohen P, Andjelkovich M, Hemmings BA. Inhibition of glycogen synthase kinase-3 by insulin mediated by protein kinase B. Nature. 1995; 378:785–789. [PubMed: 8524413]

Datta SR, Dudek H, Tao X, Masters S, Fu H, Gotoh Y, et al. Akt phosphorylation of BAD couples survival signals to the cell-intrinsic death machinery. Cell. 1997; 91:231–241. [PubMed: 9346240]

Datta SR, Katsov A, Hu L, Petros A, Fesik SW, Yaffe MB, et al. 14-3-3 proteins and survival kinases cooperate to inactivate Bad by BH3 domain phosphorylation. Mol Cell. 2000; 6:41–51. [PubMed: 10949026]

Deckworth EL, Johnson EM. Temporal analysis of events associated with programmed cell death (apoptosis) of sympathetic neurons deprived of nerve growth factor. J Cell Biol. 123:1207–1222. [PubMed: 7503996]

del Peso L, González-García M, Page C, Herrera R, Nuñez G. Interleukin-3-induced phosphorylation of BAD through the protein kinase Akt. Science. 1997; 278:687–689. [PubMed: 9381178]

Enguita M, DeGregorio-Rocasolano N, Abad A, Trullas R. Glycogen synthase kinase 3 activity mediates neuronal pentraxin 1 expression and cell death induced by potassium deprivation in cerebellar granule cells. Mol Pharmacol. 2005; 67:1237–1246. [PubMed: 15630079]

Ferriero DM. Neonatal brain injury. N Engl J Med. 2004; 351:1985–1995. [PubMed: 15525724]

Green DR, Reed JC. Mitochondria and apoptosis. Science. 1998; 281:1309–1312. [PubMed: 9721092]

Gresham GE, Alexander D, Bishop DS, Giuliani C, Goldberg G, Holland A, et al. American Heart Association Prevention Conference. IV. Prevention and Rehabilitation of Stroke. Rehabilitation Stroke. 1997; 28(7):1522–6.

Hetman M, Cavanaugh JE, Kimelman D, Xia Z. Role of glycogen synthase kinase-3beta in neuronal apoptosis induced by trophic withdrawal. J Neurosci. 2000; 20:2567–2574. [PubMed: 10729337]

Hossain MA, Russell JC, Gomez R, Laterra J. Neuroprotection by scatter factor/hepatocyte growth factor and FGF-1 in cerebellar granule neurons is phosphatidylinositol 3-kinase/Akt-dependent and MAPK/CREB independent. J Neurochem. 2002; 81:365–378. [PubMed: 12064484]

Hossain MA, Russell JC, O'Brien R, Laterra J. Neuronal pentraxin 1: a novel mediator of hypoxic-ischemic injury in neonatal brain. J Neurosci. 2004; 24:4187–4196. [PubMed: 15115814]

Johnston MV. Hypoxic and ischemic disorders of infants and children. Lecture for 38th meeting of Japanese Society of Child Neurology, Tokyo, Japan, July 1996. Brain Dev. 1997; 19(4):235–9. [PubMed: 9187471]

Kalenderian E, Pegus C, Francis C, Goodwin N, Jacques HS, Lasa D. Cardiovascular Disease urban intervention: baseline activities and findings. J Community Health. 2009; 34(4):282–7. [PubMed: 19343488]

Li F, Srinivasan A, Wang Y, Armstrong RC, Tomaselli KJ, Fritz LC. Cell-specific induction of apoptosis by microinjection of cytochrome c. Bcl-xL has activity independent of cytochrome c release. J Biol Chem. 1997a; 272:30299–30305. [PubMed: 9374516]

Li M, Wang X, Meintzer MK, Laessig T, Birnbaum MJ, Heidenreich KA. Cyclic AMP promotes neuronal survival by phosphorylation of glycogen synthase kinase 3beta. Mol Cell Biol. 2000; 20:9356–9363. [PubMed: 11094086]

Li P, Nijhawan D, Budihardjo I, Srinivasula SM, Ahmad M, Alnemri ES, et al. Cytochrome c and ATP-dependent formation of Apaf1/caspase-9 complex initiates an apoptotic protease cascade. Cell. 1997b; 91:479–489. [PubMed: 9390557]

Linseman DA, Butts BD, Precht TA, Phelps RA, Le SS, Laessig TA, et al. Glycogen synthase kinase-3β phosphorylates Bax and promotes its mitochondrial localization during apoptosis. J Neurosci. 2004; 24:9993–10002. [PubMed: 15525785]

Liu K, Lu Y, Lee JK, Samara R, Willenberg R, Sears-Kraxberger I, et al. PTEN deletion enhances the regenerative ability of adult corticospinal neurons. Nat Neurosci. 2010; 13:1075–1081. [PubMed: 20694004]

Lorenz JM, Wooliever DE, Jetton JR, Paneth N. A quantitative review of mortality and developmental disability in extremely premature newborns. Arch Pediatr Adolesc Med. 1998; 152(5):425–35. [PubMed: 9605024]

Loreto SD, Balestrino M. Development of vulnerability to hypoxic damage in *in vitro* hippocampal neurons. Int J Dev Neuroscience. 1997; 15:225–230.

Merry DE, Korsmeyer SJ. Bcl-2 gene family in the nervous system. Ann Rev Neurosci. 1997; 20:245–267. [PubMed: 9056714]

Nakajima W, Ishida A, Lange MS, Gabrielson KL, et al. Apoptosis has a prolonged role in the neurodegeneration after hypoxic ischemia in the newborn rat. J Neurosci. 2000; 20(21):7994–8004. [PubMed: 11050120]

Namura S, Zhu J, Fink K, Endres M, Srinivasan A, et al. Activation and cleavage of caspase-3 in apoptosis induced by experimental cerebral ischemia. J Neurosci. 1998; 18(10):3659–3668. [PubMed: 9570797]

Narita M, Shimizu S, Ito T, Chittenden T, Lutz RJ, Matsuda H, et al. Bax interacts with the permeability transition pore to induce permeability transition and cytochrome *c* release in isolated mitochondria. Proc Natl Acad Sci USA. 1998; 95:14681–14686. [PubMed: 9843949]

Nelson KB. Perinatal ischemic stroke. Stroke. 2007; 38:742–745. [PubMed: 17261729]

Ning K, Pei L, Liao M, Liu B, Zhang Y, Jiang W, et al. Dual neuroprotective signaling mediated by downregulating two distinct phosphatase activities of PTEN. J Neurosci. 2004; 24:4052–4060. [PubMed: 15102920]

Northington FJ, Ferriero DM, Flock DL, Martin LJ. Delayed neurodegeneration in neonatal rat thalamus after hypoxia- ischemia is apoptosis. J Neurosci. 2001a; 21(6):1931–8. [PubMed: 11245678]

Northington FJ, Ferriero DM, Martin LJ. Neurodegeneration in the thalamus following neonatal hypoxia-ischemia is programmed cell death. Dev Neurosci. 2001b; 23(3):186–91. [PubMed: 11598318]

Osredkar D, Sall JW, Bickler PE, Ferriero DM. Erythropoietin promotes hippocampal neurogenesis in in vitro models of neonatal stroke. Neurobiol Dis. 2010; 38:259–265. [PubMed: 20117210]

Oudit GY, Sun H, Kerfant BG, Crackower MA, Penninger JM, Backx PH. The role of phosphoinositide-3 kinase and PTEN in cardiovascular physiology and disease. J Mol Cell Cardiol. 2004; 37:449–471. [PubMed: 15276015]

Pérez-Pinzón MA, Xu GP, Born J, Lorenzo J, Busto R, Rosenthal M, et al. Cytochrome C is released from mitochondria into the cytosol after cerebral anoxia or ischemia. J Cereb Blood Flow Metab. 1999; 19:39–43. [PubMed: 9886353]

Pezzini, A.; Padovani, A. Cerebral ischemia in young adults: pathogenic and clinical perspectives. New York: Nova Biomedical Books; 2009.

Phiel CJ, Wilson CA, Lee VM, Klein PS. GSK-3alpha regulates production of Alzheimer's disease amyloid-beta peptides. Nature. 2003; 423:435–439. [PubMed: 12761548]

Russell JC, Whiting H, Szuflita N, Hossain MA. Nuclear translocation of X-linked inhibitor of apoptosis (XIAP) determines cell fate after hypoxia ischemia in neonatal brain. J Neurochem. 2008; 106:1357–1370. [PubMed: 18485100]

Russell JC, Kishimoto K, O'Driscoll C, Hossain MA. Neuronal pentraxin 1 induction in hypoxic-ischemic neuronal death is regulated via a glycogen synthase kinase-3α/β dependent mechanism. Cell Signal. 2011; 23:673–682. [PubMed: 21130869]

Salmena L, Carracedo A, Pandolfi PP. Tenets of PTEN tumor suppression. Cell. 2008; 133:403–414. [PubMed: 18455982]

Sharma J, Nelluru G, Wilson MA, Johnston MV, Hossain MA. Sex-specific activation of cell death signalling pathways in cerebellar granule neurons exposed to oxygen glucose deprivation followed by reoxygenation. ASN Neuro. 2011; 3(2):85–97.

Shi GD, OuYang YP, Shi JG, Liu Y, Yuan W, Jia LS. PTEN deletion prevents ischemic brain injury by activating the mTOR signaling pathway. Biochem Biophys Res Commun. 2011; 404:941–945. [PubMed: 21185267]

Shiber JR, Fontane E, Adewale A. Stroke registry: hemorrhagic vs ischemic strokes. Am J Emerg Med. 2010; 28(3):331–3. [PubMed: 20223391]

Shou Y, Li L, Prabhakaran K, Borowitz JL, Isom GE. Calcineurin-mediated Bad translocation regulates cyanide-induced neuronal apoptosis. Biochem J. 2004; 379:805–813. [PubMed: 14741051]

Smaha LA. The American Heart Association Get With The Guidelines program. Am Heart J. 2004; 148(5 Suppl):S46–8. [PubMed: 15514634]

Sudlow CL, Warlow CP. Comparable studies of the incidence of stroke and its pathological types: results from an international collaboration. International Stroke Incidence Collaboration Stroke. 1997; 28(3):491–9.

Uchino K, Billheimer D, Cramer SC. Entry criteria and baseline characteristics predict outcome in acute stroke trials. Stroke. 2001; 32(4):909–16. [PubMed: 11283391]

Volpe JJ. Perinatal brain injury: from pathogenesis to neuroprotection. Ment Retard Dev Disabil Res Rev. 2001; 7(1):56–64. [PubMed: 11241883]

Waite KA, Eng C. Protean PTEN: form and function. Am J Hum Genet. 2002; 70:B29–B44.

Wang HG, Pathan N, Ethell IM, Krajewski S, Yamaguchi Y, Shibasaki F. Ca+2-induced apoptosis through calcineurin dephosphorylation of BAD. Science. 1999; 284:339–343. [PubMed: 10195903]

Watcharasit P, Bijur GN, Song L, Zhu J, Chen X, Jope RS. Glycogen synthase kinase-3beta (GSK3beta) binds to and promotes the actions of p53. J Biol Chem. 2003; 278:48872–48879. [PubMed: 14523002]

Yang E, Zha J, Jockel J, Boise LH, Thompson CB, Korsmeyer SJ. Bad, a heterodimeric partner of Bcl-XL and Bcl-2, displaces Bax and promotes cell death. Cell. 1995; 80:285–291. [PubMed: 7834748]

Yuan J, Yankner BA. Apoptosis in the nervous system. Nature. 2000; 407:802–809. [PubMed: 11048732]

Zarotti M, Szabo I. The mitochondrial permeability transition. Biochim Biophys Acta. 1995; 1241:139–179. [PubMed: 7640294]

Zha J, Harada H, Yang E, Jockel J, Korsmeyer SJ. Serine phosphorylation of death agonist Bad in response to survival factor results in binding to 14-3-3 not Bcl-X(L). Cell. 1996; 87:619–628. [PubMed: 8929531]

Zhu Y, Hoell P, Ahlemeyer B, Krieglstein J. PTEN: a crucial mediator of mitochondria-dependent apoptosis. Apoptosis. 2006; 11:197–207. [PubMed: 16502258]

Zong WX, Lindsten T, Ross AJ, MacGregor GR, Thompson CB. BH3-only proteins that bind pro-survival Bcl-2 family members fail to induce apoptosis in the absence of Bax and Bak. Genes Dev. 2001; 15:1481–1486. [PubMed: 11410528]

Zou H, Li Y, Liu X, Wang X. An APAF-1. cytochrome c multimeric complex is a functional apoptosome that activates procaspase-9. J Biol Chem. 1999; 274:11549–11556. [PubMed: 10206961]

Highlights

- NP1 is induced in hippocampal neuronal death following OGD and HI.
- NP1 facilitates Bad and Bax translocation to mitochondria and regulates cell death.
- NP1-KO neurons showed no Bad and Bax translocation, ΔΨm and caspase-3 activation.
- Significant protection of the NP1-KO hippocampal neurons against the OGD insult.
- NP1 causes cell death by perturbing mitochondrial functions; uncover new mechanism.

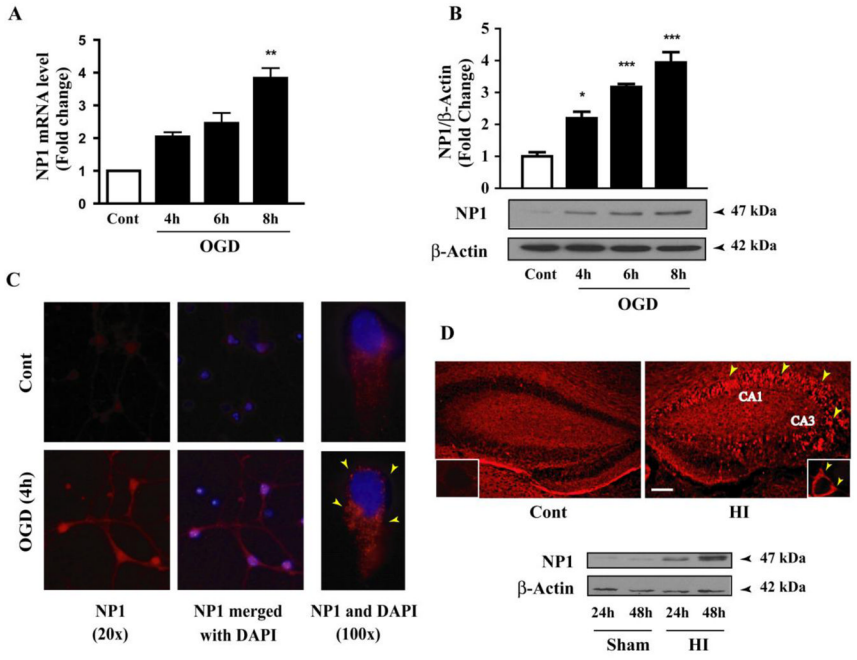

Fig. 1.

NP1 is induced in primary hippocampal cultures exposed to OGD and in the hippocampus of neonatal mice after HI. **A**) Total RNA was extracted and NP1 mRNA expression levels were analyzed by quantitative real-time PCR. Fold induction is the ratio of NP1 to internal control HPRT, which remained stable through the OGD period (values are mean±SEM, n=3; **p<0.01). **B**) Total cellular proteins were analyzed by SDS-PAGE and immunoblotted for NP1 protein. The NP1 antibody used was very specific and only detected distinct single band of molecular size at 47 kDa. Bands were quantified by densitometry and normalized to β-actin (mean±SEM, n=3; *p<0.05, ***p<0.001). **C**) Live immunostaining of cultured hippocampal neurons with NP1 specific antibody showed increased number of NP1-expressing neurons following OGD (low magnification, 20X) compared to the normoxic cultures, and neurons showing NP1 immunoreactivity at higher magnification (100X). **D**) Representative coronal brain sections (20 μm) of ipsi-, and contralateral sides of hippocampus from 48 h post-HI were analyzed for NP1-specific immunofluorescence (red) at low (10X) magnifications and at higher magnifications (100X; inset). Scale bars: 100 μm. Yellow arrows specify NP1 immunostaining. Representative Western blot image of NP1 level in the hippocampus of mice sacrificed 24 and 48 h post-HI (bottom panel). Each experiment was conducted in triplicate. Representative blots are shown.

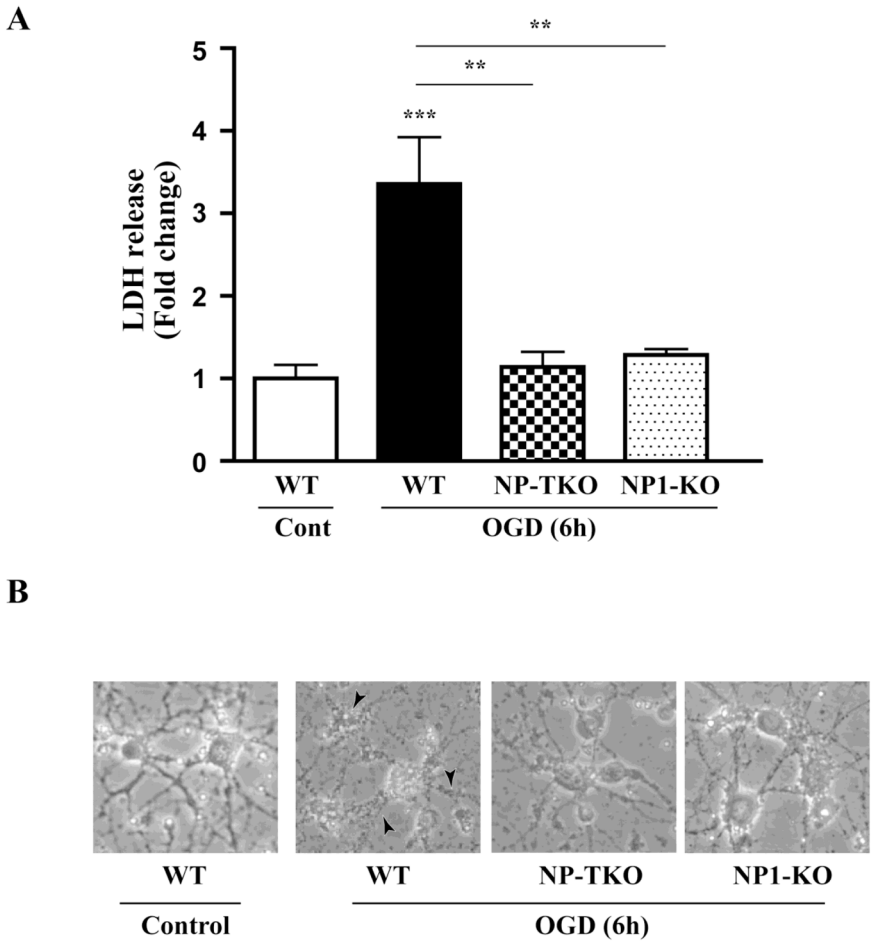

Fig. 2.

OGD exposure of WT hippocampal neurons causes cell death, while neurons from NP-TKO and NP1-KO mice are protected. **A**) Quantification of cell death by LDH release revealed OGD-induced (6h) cell death in WT but not in NP-TKO and NP1-KO hippocampal neuronal cultures. Data is expressed as LDH release normalized to normoxic controls (mean±SEM, n=6; **p<0.01, **p<0.001). **B**) Bright field morphological images of WT, NP-TKO and NP1-KO neurons exposed to OGD (6h). Black arrows indicate dying cells, and fragmented processes of the WT neurons following OGD exposure.

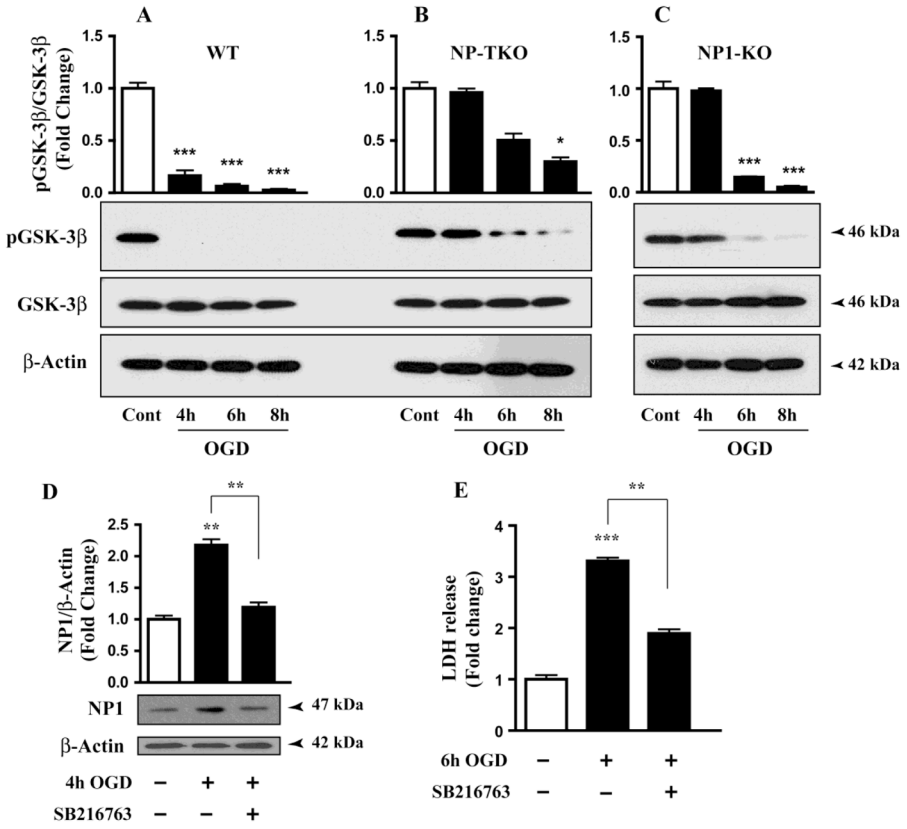

Fig. 3.

Effects of OGD exposure on the phosphorylation of GSK-3β in WT and NP-KO cultures. Total cellular proteins from WT **(A)**, NP-TKO **(B)** and NP1-KO **(C)** hippocampal cultures were immunoblotted for phospho-GSK-3β (Ser 9) and total GSK-3β using respective primary antibodies. The quantitative densitometric analyses correspond to the phospho-GSK-3β normalized to total GSK-3β. In addition, β-actin bands shown also served as a loading control. Values are mean ± SEM. (n=3; *p<0.05, ***p<0.001). **D, E**) Cells were exposed to OGD with or without pretreatment with SB216763 (10μM for 12h), a GSK-3 inhibitor. Western immunoblotting shows decrease in OGD-induced NP1-induction when pretreated with SB216763. Bands were quantified by densitometry and normalized to β-actin (mean ± SEM, n=3; **p<0.01) **(D)**. Cell cytotoxicity was measured by LDH release. Results were presented as mean ± SEM. (n=5; **p<0.01, ***p<0.001) **(E).**

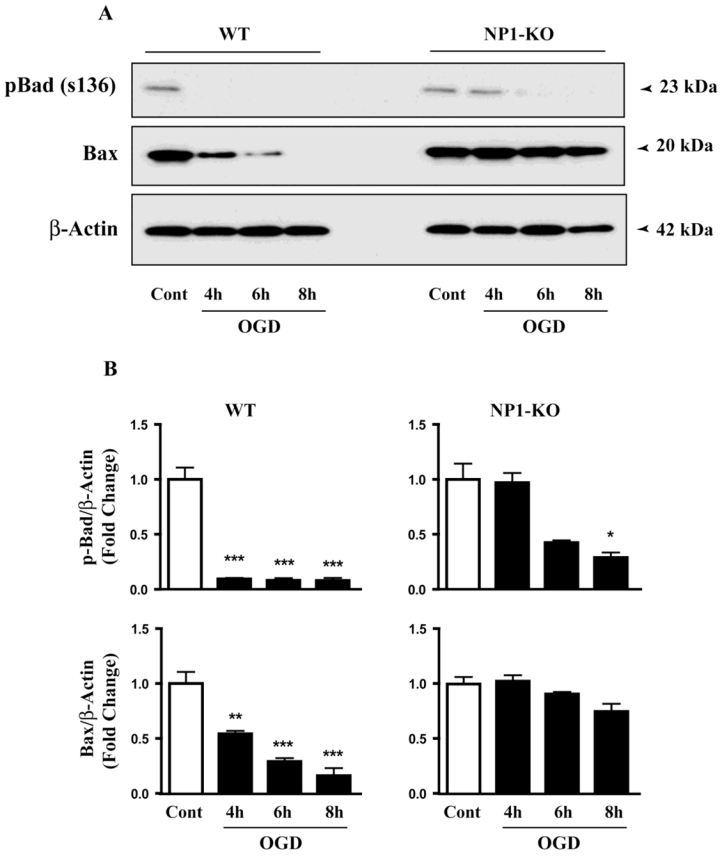

Fig. 4.

Effects of OGD on phospho-Bad and Bax in WT and NP1-KO hippocampal neuronal cultures. Total cellular proteins from WT (left panel) and NP1-KO (right panel) hippocampal cultures were analyzed by Western blot using phospho-Bad (s136) and Bax antibodies, followed by reprobing with β-actin specific antibody. (**A**) Phosphorylation of Bad and the Bax protein levels remained unchanged, at least, up to 4–6h of OGD in NP1-KO hippocampal neurons. (**B**) The quantitative densitometric analyses correspond to the phospho-Bad (s136) and Bax protein normalized to β-actin. Values are presented as mean ± SEM. (n=3; *p<0.05, **p<0.01, ***p<0.001). Representative blots are shown.

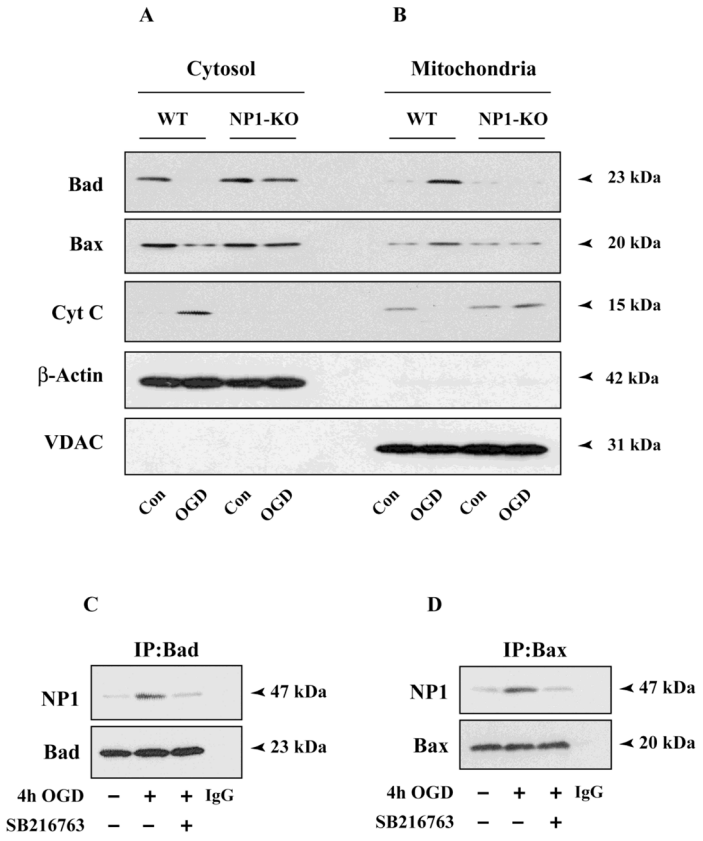

Fig. 5.

NP1 is associated with the mitochondrial translocation of Bad and Bax and subsequent Cyt C release from the mitochondria. Subcellular fractionation of total cellular extracts from WT and NP1-KO hippocampal cultures was performed following 4 h of OGD exposure. Western blot analysis showed differential distribution of Bad, Bax and Cyt C between the cytosolic (**A**) and mitochondrial (**B**) fractions from WT hippocampal cultures after OGD. In contrast, Bad, Bax and Cyt C protein levels remained unchanged in cytoplasm and mitochondrial fractions from NP1-KO cultures (**A** & **B**). VDAC and actin were used as a control for purity of the mitochondrial and cytosolic fraction, respectively, which also serve as loading controls. SDS-PAGE and immunoblotting of Bad (**C**) and Bax (**D**) immunoprecipitates from total cellular extracts revealed an OGD-induced increase in NP1 co-precipitation relative to normoxic neurons, whereas pretreatment with SB216763 (10μM for 12h) reversed the OGD-evoked increase of NP1 immunoprecipitates. IgG immunoprecipitates showed no evidence of NP1-, Bad- and Bax-specific bands. Representative blots are shown.

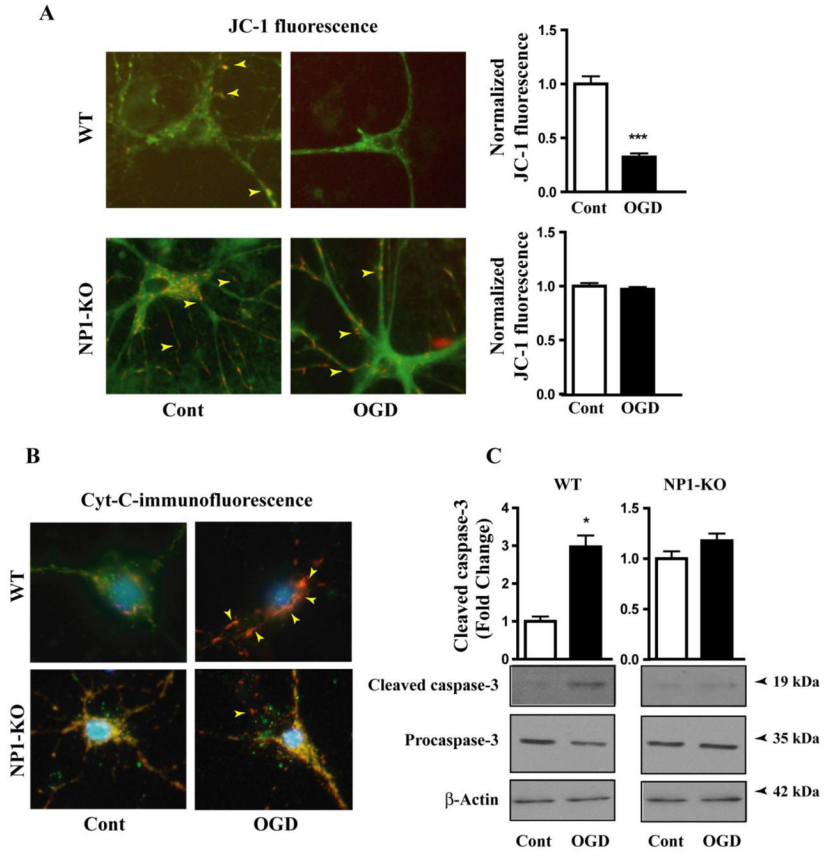

Fig. 6.

OGD induced mitochondrial membrane potential ($\Delta\Psi_m$) loss, Cyt C release, activation of caspase-3, and subsequent cell death in WT but not NP1-KO hippocampal neuronal cultures. **A**) Mitochondrial $\Delta\Psi_m$ was examined in WT and NP1-KO hippocampal neurons exposed to OGD (2h) using JC-1 fluorescence dye. OGD exposed WT cells showed significant loss of $\Delta\Psi$m (yellow arrows; ***p<0.001), but not in NP1-KO cells, compared to that in control normoxia cells. The JC-1 fluorescence was normalized as the control red-to-green ratio taken as 1. **B**) Control normoxia and OGD (4h) exposed WT and NP1−/− hippocampal neurons were immunostained with Cyt C (red), mitochondrial marker VDAC (green) and DAPI-stained nucleus of cells (blue) using respective primary antibody. Cyt C was detected predominantly in the mitochondria (yellow) in the WT control normoxia cells. OGD exposure resulted Cyt C release from mitochondria to cytosol (red) of WT hippocampal neurons but no Cyt C release was evident in NP1−/− neurons after OGD. Arrows show Cyt C-specific immunofluorescence. **C**) Western immunoblot of total cellular proteins from WT (left) and NP1-KO (right) hippocampal neurons using cleaved and procaspase-3 specific antibodies detected increased cleaved caspase-3 immunoreactive protein band in WT neurons. In contrast, cleaved caspase-3 specific band remained at the basal levels in NP1-KO cultures as compared to normoxia controls. β-actin band was visualized as loading control. Values are presented as mean ± SEM. (n=3; *p<0.05, ***p<0.001). Representative blots are shown.

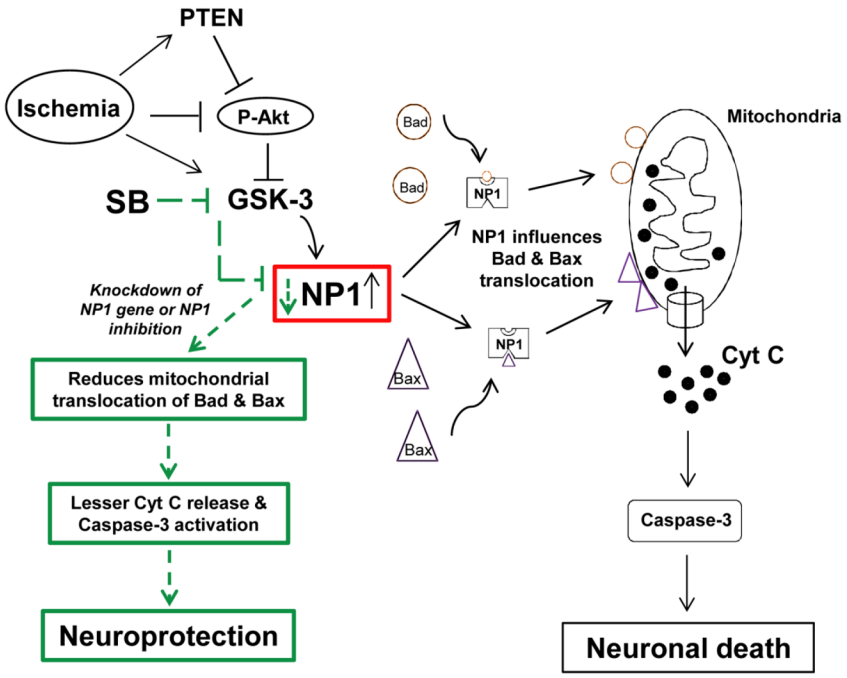

Fig. 7.

Schematic diagram proposing a potential NP1-mediated mitochondrial cell death mechanism. Ischemia causes inactivation of Akt by activating PTEN followed by GSK-3 stimulation, which induces NP1 expression. NP1 promotes apoptotic pathways by facilitating the mitochondrial translocation of Bad and Bax, thereby releasing Cyt C into the cytosol, ensuing caspase-3 activation and cell death. Inhibiting NP1 expression by using a GSK-3 inhibitor SB (SB216763) or knocking down of NP1 gene provides neuroprotection (shown in green) by preventing mitochondrial Bad/Bax translocation, Cyt C release and caspase-3 activation evoked by OGD.